Investigating the Impact of Antenna Heights on Path Loss Models in an Indoor Corridor Environment

Mohamed K. Elmezughi
EECE Department
University of KwaZulu-Natal
Durban, South Africa
m.k.elmezughi@gmail.com

Thomas J. Afullo
EECE Department
University of KwaZulu-Natal
Durban, South Africa
Afullot@ukzn.ac.za

Nicholas O. Oyie
EECE Department
University of KwaZulu-Natal
Durban, South Africa
noyie@mmust.ac.ke

***Abstract*— Mobile data traffic has rapidly increased in the last few years because of the continuous demand for higher data rates through a rapidly growing number of connected devices and the advancing technology of smartphones. Consequently, researchers have focused on frequency bands greater than 6 *GHz* because of their ability to meet the requirements of the upcoming fifth-generation (5G) wireless system, and other multimedia services that support high-speeds up to several gigabits per second. This research paper presents propagation measurements that have been conducted in a typical indoor corridor environment for both line-of-sight (LOS) and non-line-of-sight (NLOS) communication scenarios at three frequencies in the super high frequency (SHF) band, which are 14, 18, and 22 *GHz*. Moreover, this work aims primarily to investigate the effect of changing the antenna height on the performance of two well-known path loss prediction models. The models considered in this work are the close-in (CI) free space reference distance model and the floating-intercept (FI) model. Furthermore, this study presents mean square error (MSE) between the same and different antenna heights. The results observed that the CI model provides more stability than the FI model at the frequency bands selected in the LOS communication scenario. In contrast, both models have comparable performance in the NLOS scenario. Furthermore, the 22 *GHz* frequency band has attractive behavior since the impact of the antenna's height is negligible at this band compared to 14 and 18 *GHz* frequency bands at both the CI and FI models in the LOS and NLOS scenarios. Finally, the results show that both models are suitable for predicting path loss in enclosed environments like corridors.**

Keywords—mmWave, path loss, propagation measurements, antenna height, indoor corridor.

I. INTRODUCTION

The rapid increase in mobile data traffic accelerates research on the frequency bands above 6 GHz (i.e., the super high frequency (SHF), the millimeter-wave (mmWave), and higher frequency bands) [1]-[6]. The reason behind that is to address the disability of today's centimeter-wave (cmWave or microwave) that will not meet the requirements of the fifth-generation (5G) wireless network and other multimedia services because of the scarcity of the bandwidth [1][7]-[10].

The SHF (3-30 GHz) and the mmWave (30-300 GHz) frequency bands have similar behavior and propagation characteristics, hence both called mmWave [1][11]. These bands offer amounts of continuous bandwidth that can offer high peaks of data transmission up to several gigabits per second [1][4]. However, the jump to the mmWave regime poses wireless channel characteristics and behaviors far from the microwave bands. Accordingly, accurate understanding and modeling of the mmWave channel in different outdoor and indoor environments are vital for reliable deployments of 5G system and other high-speed multimedia services [10][12]-[14].

The mmWave frequency regime was used in many high-speed applications such as the local multipoint distribution services (LMDS), radar, active and passive earth explorations, satellite communications, point-to-point communications, and in the military applications [11][15][16]. Also, the SHF band was heavily exploited by these applications.

In order to model and characterize the wireless channel at mmWave, a massive number of measurement campaigns have been carried out worldwide in different indoor and outdoor environments and scenarios. The path loss exponent (PLE) and the shadow fading (SF) standard deviation are calculated at different indoor and outdoor scenarios in the Islamic structured environments in the Arabian Peninsula at 28 GHz frequency band [4][17]. The design of buildings in those areas is different from other places in the world, and the outdoor temperature is high (usually exceeding 40 $°C$ most of the time). Extensive measurements and path loss models are presented and compared for closed plan indoor environments at 28 and 73 GHz reported in [18]. Accurate modification of the free space (FS) and the Stanford University Interim (SUI) models and directional mmWave path loss models at 28, 38, 60, and 73 GHz can be found in [19][20]. Zhang et al. [12] presented indoor measurements and characterization of the wireless channel for office, hall, and classroom scenarios at 27-29 GHz and examined the effect of the furniture in the office scenario. Comparison study of path loss models at 30, 140, and 300 GHz based on measurements in an indoor environment was reported in [10]. The PLE values of the line-of-sight (LOS), non-line-of-sight (NLOS), and obstructed LOS scenarios at the D-band (110-170 GHz) are presented in [21]. Other studies that were considered in the literature review for various indoor environments include corridors [1]19][20], dining room [7], laboratories and classrooms [7][12][23], halls [7][24], offices [7][18][24], and shopping malls [25].Related works in outdoor environments can be found in [3][11][13][18][26]-[33].

Oyie and Afullo [1] presented path loss prediction models based on real measured data collected in an indoor corridor environment at 14, 18, and 22 GHz for both LOS and NLOS scenarios. This study mainly focused on comparing the close-in (CI) free space reference distance model with the dual-slope (DS) CI model. The results of this work show that the DS model has better performance than the CI model in terms of fitting the real measured data and minimizing the standard deviation of the SF. The same authors have extended this work

978-1-7281-6770-1/20/$31.00 ©2020 IEEE

in [22] by comparing the DS model with the alpha-beta-gamma (ABG) model considering the waveguiding effect, modal attenuation of signal strength, and the propagation mechanisms such as diffraction and reflection. This study performed at the same frequency bands in two different indoor corridor environments, which are concrete-based corridor and glass-based corridor. The outcome reveals that both the ABG and the DS CI path loss prediction models are suitable for indoor environments due to their accuracy of fitting the real measured data with lower values of the SF standard deviation in the ABG model.

In [14], LOS probability and omnidirectional path loss models were presented for indoor corridor environments at 18 GHz frequency band taking into consideration materials and the structure of the indoor corridor. The proposed models improved the accuracy of the existing models and offered reliable omnidirectional models for indoor wireless communications. However, the previous works did not investigate and highlight how these models behave when the antenna height changes. Consequently, this paper tries to fill this gap by presenting the performance of the well-known CI model and the floating-intercept (FI) model in terms of changing the transmitter (Tx) antenna height based on real measured data that have been collected. Also, this study investigates the sensitivity and stability of the models' parameters according to that for both LOS and NLOS communication scenarios at 14, 18, and 22 GHz in an indoor corridor environment.

The rest of this paper is organized as follows. The description of the measurement campaigns is given in Section II. The path loss models adopted in this study are presented and briefly derived in Section III. The results and discussions are provided in section IV. Finally, the conclusion of this work is presented in Section V.

II. MEASUREMENT CAMPAIGNS DESCRIPTION

This section describes the measurement campaigns that have been conducted on the 5th floor of the Electrical, Electronic, and Computer Engineering (EECE) Department, University of KwaZulu-Natal, Howard College Campus, Durban, South Africa. These measurements have been carried out, aiming to model and investigate the path loss for both LOS and NLOS communication scenarios at three frequency bands above 6 GHz, which are 14, 18, and 22 GHz.

A. *Channel Sounder and Measurements Setup*

The wireless channel sounder utilized in the measurement campaigns consists of Rohde and Schwarz SMF 100A Signal Generator, Rohde and Schwarz FSIQ 40 Signal Analyzer with a frequency range from 20 Hz to 40 GHz and a maximum working bandwidth of 120 MHz, two identical high-gain antennas, and coaxial cables and connectors. Fig. 1 shows the channel sounder adopted in these measurement campaigns.

The type of the transmitting and receiving antennas used is directional pyramidal horn antennas with a directional gain equal to19.5°, 20.95°, and 22.1° at 14, 18, and 22 GHz, respectively. The antennas have a half-power beamwidth (HPBW) values ranging from 13° to 19.2° and from 15° to 18.4° in the elevation and azimuth plans, respectively. Two practical transmitting antenna heights have been considered in the measurements, which are 1.6 m and 2.3 m above the floor level, whereas the height of the receiving antenna was fixed at 1.6 m above the floor level. The polarization of the antennas is vertical. Table I provides a detailed summary of the measurements setup considered in this work.

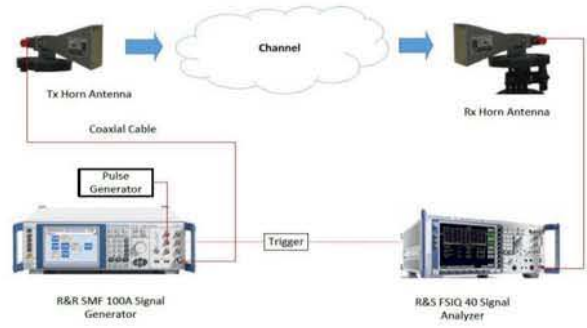

Fig. 1: The architecture of the channel sounder.

TABLE I. MEASUREMENTS SETUP AND CONFIGURATIONS

Parameter	Configuration	Units
Center Frequency	14, 18, and 22	GHz
Bandwidth	100	MHz
Transmitted Signal	Continuous	-
Tx and Rx Antenna Type	Direc. Horn Ant.	-
Transmitted Power	10	dBm
Tx Antenna Height	1.6 and 2.3	m
Rx Antenna Height	1.6	m
Antennas Polarization	Vertical	-
Antennas Gain at 14 GHz	19.5	dBi
Antennas HPBW at 14 GHz	Azim. 18.4°, Elev. 19.2°	Degree
Antennas Gain at 18 GHz	20.95	dBi
Antennas HPBW at 18 GHz	Azim. 15.4°, Elev. 15.6°	Degree
Antennas Gain at 22 GHz	22.1	dBi
Antennas HPBW at 22 GHz	Azim. 15°, Elev. 13°	Degree

B. *Measurements Scenario and Experimental Procedures*

The measurement environment is a typical indoor corridor with dimensions equal to 30 m, 1.4 m, and 2.63 m for the length, width, and height, respectively. The corridor is made of dry concrete and bricks, and contains an elevator, a staircase, and wooden doors for offices. The measurements have been carried by moving the Rx antenna away from the Tx antenna starting from 2 m Tx-Rx separation distance until 24 m with incremental steps of 2 m. The number of the Tx-Rx separation distances is 13 considering the reference distance d_0=1 m. For every single step, 10 dBm transmitted signals from the signal generator received by the signal analyzer for both LOS and NLOS communication scenarios at 14, 18, and 22 GHz frequency bands.

The LOS scenario considered when both antennas aligned on boresight without any obstacle in the transmitting signal path between them. For the NLOS scenario, no obstacles were considered in the wireless channel between the Tx and Rx antenna, however, the antennas are misaligned, and the Rx antenna was rotating in the azimuth plane by 10° incremental steps having 36 angles of arrival (AoA). This procedure was

repeated for two typical Tx antenna heights, which are 1.6 m and 2.3 m above the floor level. The Receiver relied mainly on reflections and diffractions to catch the signal, as shown in Fig. 2 that represents the floor plan of the indoor corridor adopted in this study. More details about the measurements can be found in [1][14][22].

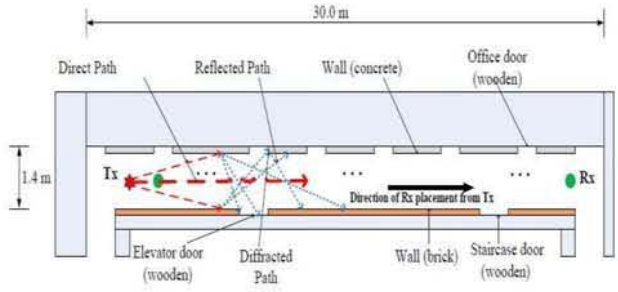

Fig. 2: Floor plan of the indoor corridor environment.

III. PATH LOSS PREDICTION MODELS

Designing and analyzing reliable communication systems in terms of the prediction of signal strength and link budget need to have accurate path loss prediction models covering all potential communication scenarios in all indoor and outdoor environments.

The path loss represents the reduction of the signals' power as it travels through the wireless communication channel between the transmitting and receiving antennas. Thus, this primary parameter causes the contraction of the cell coverage area and affects the signal-to-noise plus interference ratio (SNIR) and the data transmission rates [1]. Modeling the large-scale path loss can be achieved deterministically, stochastically, or empirically. However, the characterization of the wireless propagation channels based on measurements is more comfortable and reliable [3][30]. This section presents a full description and derivation of two well-known path loss prediction models, which are the CI and FI models.

All the existing path loss models can be derived starting from the Friis equation, which represents the free space path loss between two isotropic antennas aligned on boresight (i.e., LOS path between the antennas without any obstacle in between). The free space path loss (FSPL) depends mainly on the operating frequency and the Tx-Rx separation distance, as expressed in Eq. (1)

$$FSPL(f,d) = \left(\frac{4\pi df}{c}\right)^2, \quad (1)$$

where d is the Tx-Rx separation distance in meters, f is the operating frequency, and c is the speed of light in the free space which is approximately equal to $3 \times 10^8\ m/s$. Eq. (1) can be expressed in decibel's units considering d and f as variables, as shown in Eq. (2)

$$FSPL(f,d) = k + 2 \times 10\log_{10}(d) + 2 \times 10\log_{10}(f), \quad (2)$$

where k is a constant considering the value of $\frac{4\pi}{c}$ after converting it to the decibel's scale. For single-frequency path loss modeling, the term $2 \times 10\log_{10}(f)$ is a constant, then

$$FSPL(f,d) = k_1 + 2 \times 10\log_{10}(d), \quad (3)$$

where k_1 is a coefficient in dB. The path loss dependency on the operating frequency is included in k_1. Note that from Eq. (3), the value 2 is the PLE of the free space. However, this value will be changed because of the wireless channel characteristics (reflections, diffractions, scattering, etc.) and the communication scenario (i.e., LOS or NLOS). In general, the value of the PLE in the LOS scenario is smaller than the values in the NLOS scenario. Also, the value of this critical parameter is less than 2 for indoor environments and greater than 2 for outdoor environments. Eq. (3) can be generalized to represent the path loss for every climate and communication scenario from the following formula

$$PL(d) = k_1 + k_2 \times 10\log_{10}(d), \quad (4)$$

where k_2 is the PLE (also called power decay index), which is a $unitless$ coefficient that describes the path loss behavior with the Tx-Rx separation distance. Depending on the principle used to calculate the value of coefficients k_1 and k_2. There are many path loss models. We adopted the CI and FI models in this work. The path loss from the link budget as a function of the transmitted power (P_t), received power (P_r), transmitting antenna gain (G_t), and receiving antenna gain (G_r) is given by

$$PL(d) = P_t - P_r(d) + G_t - G_r. \quad (5)$$

Note that the received power in Eq. (5) depends on the Tx-Rx separation distance. Also, the previous equation is used to have the measured path loss values by knowing the Rx signal levels detected by the signal analyzer.

A. *The CI Path Loss Prediction Model*

The CI model can be expressed from Eq. (4) by replacing k_1 and k_2 by the FSPL at a particular reference distance d_0 and the PLE (n), respectively. The reference distance of the CI model adopted in this study is 1 m. Standardizing the reference distance of the CI model makes it easier to compare various frequency bands and works of other researchers, and enables closed-form computation in the analysis [11]. The reason for using 1 m as a reference distance for both LOS and NLOS scenarios in the measurement campaigns is that the SHF and mmWave bands present a significant variety of path loss values within the first meter of propagation away from the transmitter [11]. After considering the SF that describes the signal fluctuations because of shadowing and other effects that affect the propagation signals traveling through the transmission channel, the CI model can be expressed by the following equation

$$PL_{CI}(d) = FSPL(f,1m) + 10nlog_{10}(d) + X_\sigma^{CI}, \quad (6)$$

where $FSPL(f,1m)$ is the value of the FSPL at the operating frequency and reference distance $d_0 = 1m$, n represents the PLE, and X_σ^{CI} is the SF Gaussian random variable with zero mean and standard deviation σ. The minimum mean square error (MMSE) technique is used to find the parameters of the CI model (i.e., n and σ).

B. *The FI Path Loss Prediction Model*

The FI model can be expressed from Eq. (4) by replacing k_1 and k_2 by the parameters α and β, respectively. The full equation of the FI model is given by

$$PL_{FI}(d) = \alpha + 10\beta log_{10}(d) + X_{\sigma}^{FI}, \qquad (7)$$

where α and β are the floating-intercept and the slope of the path loss line. These parameters, unlike the CI model's parameter that depends on the physical anchor that catches the path loss value near Tx, the FI model depends on the mathematical curve that fits the real measured data. The parameter β is equal to the PLE if and only if α equal to the value of FSPL at the reference distance (d_0). The MMSE approach is used to find the parameters of the FI model (i.e., α, β, and X_{σ}^{FI}).

IV. RESULTS AND DISCUSSIONS

This section presents the results and discussions of investigating the effect of changing antenna height on the parameters of the path loss prediction models considered at 14, 18, and 22 GHz for both LOS and NLOS communication scenarios. This study has been motivated by knowing that the behavior of the wireless channel after 6 GHz (i.e., SHF and mmWave frequency regime) is different from today's 4G microwave frequency bands. Considering and investigating two practical heights provides reliable path loss models and a vision of how the wireless channel in enclosed environments such as corridors behaves in terms of their stability and dependency. Figures 3 and 4 represent the CI and FI path loss models for the LOS scenario at 14, 18, and 22 GHz, respectively. It reveals that from figures 3 and 4, the CI model provides more stability than the FI model, and the effect of antenna height is minimum at 22 GHz frequency band. It can be seen in figures 5 and 6 that the mean square error (MSE) between the same and different antennas height ranging between 10^{-4} and 10^{-2} for the CI model and from 10^{-2} to 10^{-1} for the FI model. The MSE curves reveal that the CI model parameters are less sensitive than the FI model parameters in terms of changing the antenna heights. The increasing range of the PLE due to changing the Tx antenna height is from 3.32% to 7.27% of its value when both antennas have the same height. Table II shows the parameters' values of the path loss models at 14, 18, and 22 GHz for the LOS scenario. It is notable from Table II that the standard deviation of the SF has a rapid increase because of antennas' height mismatching.

TABLE II. LOS COMMUNICATION SCENARIO RESULTS

	Frequency Bands and Tx Antenna Heights					
	14 GHz		***18 GHz***		***22 GHz***	
	1.6 m	***2.3 m***	***1.6 m***	***2.3 m***	***1.6 m***	***2.3 m***
PLE (n)	1.372	1.416	1.584	1.699	1.658	1.714
σ_{min}^{CI} **[dB]**	2.190	5.369	1.534	1.997	1.312	4.801
α_{FI} **[dB]**	55.44	61.83	57.48	59.07	61.04	67.63
β_{FI}	1.365	0.823	1.590	1.563	1.503	0.970
σ_{min}^{FI}**[dB]**	2.190	4.359	1.534	1.904	1.117	3.489

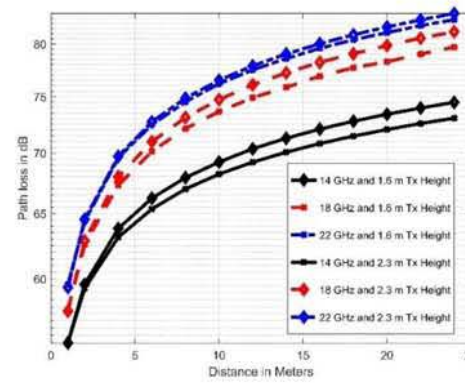

Fig. 3: The CI LOS path loss prediction model at three frequency bands and two antenna heights.

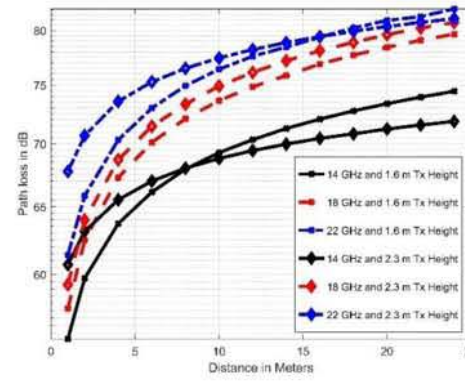

Fig. 4: The FI LOS path loss prediction model at three frequency bands and two antenna heights.

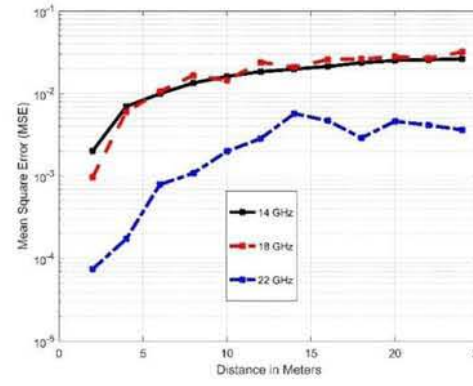

Fig. 5: The MSE between two CI LOS path loss prediction models with different antenna heights at three frequency bands.

Figures 7 and 8 show the CI and FI path loss models for the NLOS scenario at 14, 18, and 22 GHz, respectively. It can be noted that for the NLOS scenario, the PLE value changes by 7.35% to 0.69% at 14 and 22 GHz. Also, it is clear from figures 7 and 8 that the 18 GHz band has the worst performance in both CI and FI models since their curves move away from each other at this frequency band as the Tx-Rx separation distance increased. Moreover, from both of the figures, it can be seen that the 22 GHz frequency band has the highest path loss value. The MSE plots at the three frequency bands for the NLOS communication scenario are represented

in figures 9 and 10. For the NLOS scenario, the variation of the standard deviation is quite small compared to the LOS scenario. This is due to the waveguiding effect, and the richness of reflections and diffraction, making constructive interference of the multiple signal components reached the Rx side in both cases (i.e., same and different antenna heights). For both the LOS and NLOS scenarios, the 22 GHz frequency band has attractive behavior in terms of it being less sensitive to changes in antenna height in both the CI and FI models. Variation of antenna height changes the angle of incidence of the transmitted signals on the obstacles in the proximity of the receiver antenna. At higher frequency (22 GHz), or smaller wavelengths, the results suggest that the changes in angles of the incident have insignificant effects on the reflected signals. Future generation networks will be deployed in small cells due to high path loss at frequencies above 6GHz. The expected points of fixing the transmitter antenna are ceiling and lamp posts in indoors and outdoors, respectively. The heights of the transmitter antennas are likely to vary depending on the nature of the deployment scenario. Table III summarizes the NLOS parameters of the CI and FI path loss models at three frequencies with two different Tx antenna heights.

This work will be extended to cover higher frequency bands in different communication scenarios. This technique will open the scope for having improved path loss prediction models that take into account the hight of the Tx and Rx antennas. Hence, providing more precision in predicting the path loss for systems' design and link budget calculations.

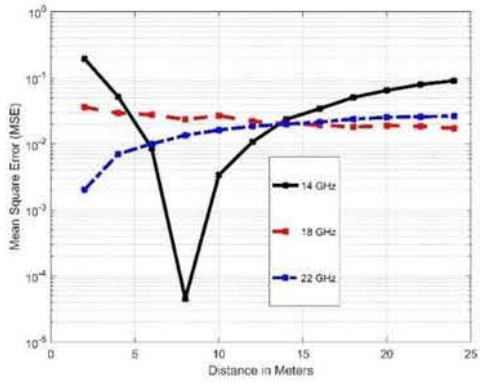

Fig. 6: The MSE between two FI LOS path loss prediction models with different antenna heights at three frequency bands.

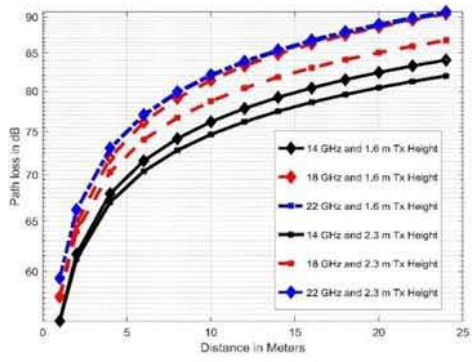

Fig. 7: The CI NLOS path loss prediction model at three frequency bands and two antenna heights.

TABLE III. NLOS COMMUNICATION SCENARIO RESULTS

	Frequency Bands and Tx Antenna Heights					
	14 GHz		***18 GHz***		***22 GHz***	
	1.6 m	***2.3 m***	***1.6 m***	***2.3 m***	***1.6 m***	***2.3 m***
PLE (n)	2.073	1.921	2.377	2.109	2.259	2.274
σ_{min}^{CI} **[dB]**	5.984	6.022	6.866	6.593	6.858	7.150
α_{FI} **[dB]**	67.27	66.52	71.02	70.16	73.24	73.78
β_{FI}	1.010	0.926	1.172	0.964	1.014	0.982
σ_{min}^{FI}**[dB]**	3.693	4.091	4.318	4.194	4.075	4.279

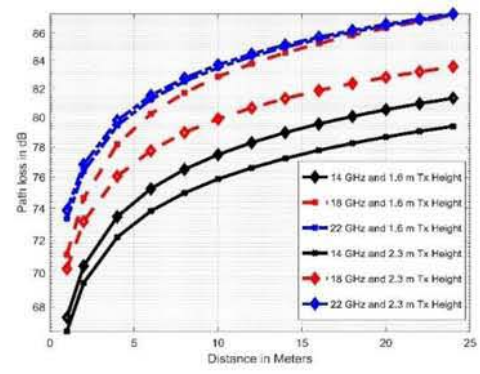

Fig. 8: The FI NLOS path loss prediction model at three frequency bands and two antenna heights.

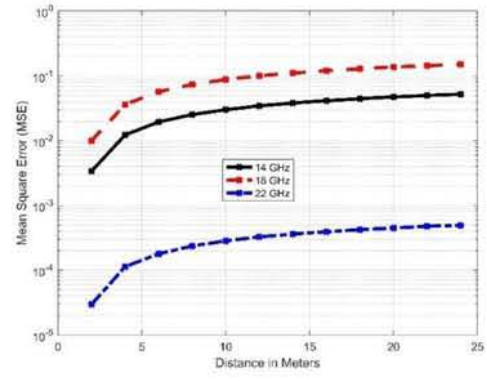

Fig. 9: The MSE between two CI NLOS path loss prediction models with different antenna heights at three frequency bands.

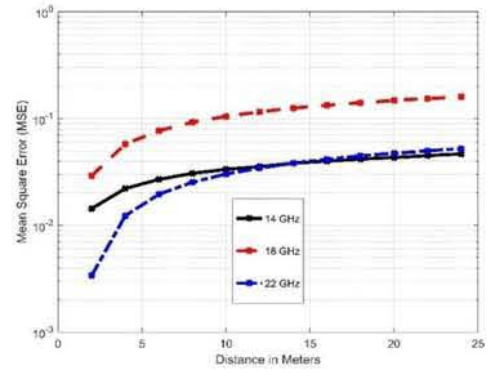

Fig. 10: The MSE between two FI NLOS path loss prediction models with different antenna heights at three frequency bands.

V. Conclusion

In this paper, measurement campaigns have been carried out to investigate the effect of the antenna height on the performance of the CI and FI path loss prediction models. The measurements' environment was an indoor corridor on the 5th floor of the Electrical, Electronic, and Computer Engineering (EECE) Department, University of KwaZulu-Natal, Howard College Campus, South Africa. The measurements were performed for both the LOS and NLOS communication scenarios at three frequency bands above 6 GHz, which are 14, 18, and 22 GHz. The LOS results reveal that the CI model offers more stability than the FI model at the frequency bands selected. For the NLOS scenario, both models have the same sensitivity to the change of antenna height. Moreover, the results show that both models have a notable increase in the SF standard deviation when compared with the NLOS. In addition, it is clear from the results that the effect of antenna height is negligible at 22 GHz frequency band for both the CI and FI models in the LOS and NLOS scenarios. Finally, the CI model can be trusted as an accurate and stable path loss model for enclosed environments such as corridors. Further studies that investigate the impact of the angle of arrival and the antennas' height on the performance of improved path loss models based on measurements will be carried out in future works.

References

[1] N. O. Oyie and T. J. O. Afullo, "Measurements and analysis of large-scale path loss model at 14 and 22 GHz in indoor corridor," IEEE Access, vol. 6, pp. 17205–17214, Feb. 2018.

[2] L. Pometcu and R. D'Errico, "An Indoor Channel Model for High Data Rate Communications in D-Band," IEEE Access, vol. 8, pp. 9420–9433, Dec. 2019.

[3] M. Aborahama, A. Zakaria, M. H. Ismail, M. El-Bardicy, M. El-Tarhuni, and Y. Hatahet, "Large-scale channel characterization at 28 GHz on a university campus in the United Arab Emirates," Telecommun. Sys., vol. 1, pp. 1–15, Jan. 2020.

[4] F. Hossain, T. K. Geok, T. A. Rahman, M. N. Hindia, K. Dimyati, and A. Abdaziz, "Indoor millimeter-wave propagation prediction by measurement and ray tracing simulation at 38 GHz," Symmetry, vol. 10, p.464, Oct. 2018.

[5] X. Wu, C. X. Wang, J. Sun, J. Huang, R. Feng, Y. Yang, and X. Ge, "60-GHz millimeter-wave channel measurements and modeling for indoor office environments," IEEE Trans. Antennas Propag., vol. 65, pp. 1912–1924, Feb. 2017.

[6] T. Kleine-Ostmann, C. Jastrow, S. Priebe, M. Jacob, T. Kürner, and T. Schrader, "Measurement of channel and propagation properties at 300 GHz" 2012 Conf. Precision electromagn. Measurements, Jul. 2012, pp. 258–259.

[7] A. M. Al-Samman, T. A. Rahman, M. H. Azmi, and S. A. Al-Gailani, "Millimeter-wave propagation measurements and models at 28 GHz and 38 GHz in a dining room for 5G wireless networks," Measurement, vol. 130, pp. 71–81, Dec. 2018.

[8] G. R. MacCartney, H. Yan, S. Sun, and T. S. Rappaport, "A flexible wideband millimeter-wave channel sounder with local area and NLOS to LOS transition measurements," 2017 IEEE Int. Conf. Commun. (ICC), May. 2017, pp. 1–7.

[9] A. Zhou, J. Huang, J. Sun, Q. Zhu, C. X. Wang, and Y. Yang, "60 GHz channel measurements and ray tracing modeling in an indoor environment," 2017 9th Int. Con. Wireless Commun. Signal Proces. (WCSP), vol. 63, no. 9, pp. 3029–3056, May. 2015.

[10] C. L. Cheng, S. Kim, and A. Zaji´c, "Comparison of path loss models for indoor 30 GHz, 140 GHz, and 300 GHz channels," 2017 11th European Conf. Antennas Propag. (EUCAP), Mar. 2017, pp. 716–720.

[11] T. S. Rappaport, G. R. MacCartney, M. K. Samimi, and S. Sun, "Wideband millimeter-wave propagation measurements and channel models for future wireless communication system design," IEEE Trans. Commun., Oct. 2015, pp. 1–6.

[12] G. Zhang, K. Saito, W. Fan, X. Cai, P. Hanpinitsak, J. I. Takada, and G. F. Pedersen, "Experimental characterization of millimeter-wave indoor propagation channels at 28 GHz," IEEE Access, vol. 6, pp. 76516–76526, Nov. 2018.

[13] G. R. MacCartney, and J. Zhang, S. Nie, and T. S. Rappaport, "Path loss models for 5G millimeter wave propagation channels in urban microcells," Globecom, pp. 3948–3953, Dec. 2013.

[14] N. O. Oyie and T. J. O. Afullo, "An Empirical Approach to Omnidirectional Path Loss and Line-of-sight Probability Models at 18 GHz for 5G Networks," 2018 Prog. Electromagn. Res. Symp. (PIERS-Toyama), Aug. 2018, pp. 129–136.

[15] T. S. Rappaport, Y. Xing, G. R. MacCartney, A. F. Molischand, E. Mellios, and J. Zhang, "Overview of millimeter wave communications for fifth generation (5G) wireless networks—With a focus on propagation models," IEEE Trans. Antennas Propag., vol. 65, no. 12, pp. 6213–6230, Aug. 2017.

[16] A. Osseiran, J. F. Monserratand and P. Marsch, "5G mobile and wireless communications technology," Int. J. Satell. Commun. and Networ., vol. 34, no. 3, pp. 351-360, May. 2016.

[17] Y. Hatahet, A. Zakaria, M. Ismail, M. El-Tarhuni "Large-scale channel measurements at 28 GHz in the United Arab Emirates for 5G systems," IEEE Radio and Wireless Symposium (RWS), Jan. 2019, pp. 1--4.

[18] T. S. Rappaport, S. Sun, M. Rimma, H. Zhao, and Y. Azar, K. Wang, G. N. Wong, J. K. Schulz, M. Samimi, and F. Gutierrez, "Millimeter wave mobile communications for 5G cellular: It will work!," IEEE Access, vol. 1, pp. 335–349, May. 2013.

[19] A. I. Sulyman, A. Alwarafy, G. R. MacCartney, T. S. Rappaport, and A. Alsanie, "Directional radio propagation path loss models for millimeter-wave wireless networks in the 28-, 60-, and 73-GHz bands," IEEE Trans. Wireless Commun., vol. 15, no. 10, pp. 6939–6947, Jul. 2016.

[20] A. I. Sulyman, A. T. Nassar, M. K. Samimi, G. R. MacCartney, T. S. Rappaport, and A. Alsanie, "Radio propagation path loss models for 5G cellular networks in the 28 GHz and 38 GHz millimeter-wave bands," IEEE Commun. Mag., vol. 52, no. 9, pp. 78–86, Sep. 2014.

[21] S. Kim, W. T. Khan, A. Zaji´c, and J. Papapolymerou, "D-band channel measurements and characterization for indoor applications," IEEE Trans. Antennas Propag., vol. 63, no. 7, pp. 3198–3207, Apr. 2015.

[22] N. O. Oyie and T. J. O. Afullo, "A Comparative Study of Dual-Slope Path Loss Model in Various Indoor Environments at 14 to 22 GHz," 018 Prog. Electromagn. Res. Symp. (PIERS-Toyama), Aug. 2018, pp. 121–128.

[23] X. Wu, Y. Zhang, C. Wang, G. Goussetis, and M. Alwakeel, "28 GHz indoor channel measurements and modelling in laboratory environment using directional antennas,", 9th European Conf. Antennas Propag. (EuCAP), IEEE, April. 2015, pp. 1--5.

[24] A. M. Al-Samman, T. Abd Rahman, and M. H. Azmi, "Indoor corridor wideband radio propagation measurements and channel models for 5G millimeter wave wireless communications at 19 GHz, 28 GHz, and 38 GHz Bands," Wireless Commun. Mobile Comp., vol. 2018, 2018.

[25] S. L. Nguyen, J. Jarvelainen, Karttunen, A. K. Haneda,. and J. Putkonen, ''Comparing radio propagation channels between 28 and 140 GHz bands in a shopping mall,'', IET, pp. 505–515, 2018.

[26] Y. Azar, G. N. Wong, K. Wang, R. Mayzus, J. K. Schulz, H. Zhao, F. Gutierrez, D. Hwang, and T. S. Rappaport, "28 GHz propagation measurements for outdoor cellular communications using steerable beam antennas in New York City," 2013 IEEE Int. Conf. Commun. (ICC), Jun. 2013, pp. 5143–5147.

[27] S. Sun, G. R. MacCartney, and T. S. Rappaport, "Millimeter-wave distance-dependent large-scale propagation measurements and path loss models for outdoor and indoor 5G systems," 2016 10th European Conf. Ant. Propag. (EuCAP), Apr. 2016, pp. 1–5.

[28] A. F. Molisch, A. Karttunen, R. Wang, and C. U. Bas, S. Hur, J. Park, and J. Zhang, "Millimeter-wave channels in urban environments," IEEE 5G Tech. Focus, Apr. 2016, pp. 1–5.

[29] S. Sun, T. S. Rappaport, T. A. Thomas, A. Ghosh, H. C. Nguyen, I. Z. Kovács, I. Rodriguez, O. Koymen, and A. Partyka, "Investigation of prediction accuracy, sensitivity, and parameter stability of large-scale propagation path loss models for 5G wireless communications," IEEE Trans. Veh. Tech., vol. 65, no. 5, pp. 2843–2860, Mar. 2016.

[30] G. R. MacCartney, and T. S. Rappaport, "73 GHz millimeter wave propagation measurements for outdoor urban mobile and backhaul communications in New York City," IEEE Int. conf. Commun. (ICC), Jun. 2014, pp. 4862–4867.

[31] M. K. Samimi and T. S. Rappaport, "Ultra-wideband statistical channel model for non line of sight millimeter-wave urban channels," 2014 IEEE Global Commun. Conf., Dec. 2014, pp. 3483–3489.

[32] T. S. Rappaport, F. Gutierrez, E. Ben-Dor, J. N. Murdock, Y. Qiao, and J. I. Tamir, "Broadband millimeter-wave propagation measurements and models using adaptive-beam antennas for outdoor urban cellular communications," IEEE trans. Antennas Propag., vol. 61, no. 4, pp. 1850–1859, Dec. 2012.

[33] D. He, B. Ai, K. Guan, Z. Zhong, and B. Hui, J. Kim, H. Chung, and I. Kim, "Channel measurement, simulation, and analysis for high-speed railway communications in 5G millimeter-wave band," IEEE Trans. Intel. Transp. Systems, vol. 19, no. 10, pp. 3144–3158, Dec. 2017.